Available online at www.sciencedirect.com
SCIENCE DIRECT®
Journal of Sound and Vibration 278 (2004) 589–610
JOURNAL OF SOUND AND VIBRATION
www.elsevier.com/locate/jsvi

Structural damage identification of the highway bridge Z24 by FE model updating

A. Teughels*, G. De Roeck

Division of Structural Mechanics, Department of Civil Engineering, Katholieke Universiteit Leuven, Kasteelpark Arenberg 40, B-3001 Heverlee, Belgium

Received 30 April 2003; accepted 13 October 2003

Abstract

The development of a methodology for accurate and reliable condition assessment of civil structures has become very important. The finite element (FE) model updating method provides an efficient, non-destructive, global damage identification technique, which is based on the fact that the modal parameters (eigenfrequencies and mode shapes) of the structure are affected by structural damage. In the FE model the damage is represented by a reduction of the stiffness properties of the elements and can be identified by tuning the FE model to the measured modal parameters. This paper describes an iterative sensitivity based FE model updating method in which the discrepancies in both the eigenfrequencies and unscaled mode shape data obtained from ambient tests are minimized. Furthermore, the paper proposes the use of damage functions to approximate the stiffness distribution, as an efficient approach to reduce the number of unknowns. Additionally the optimization process is made more robust by using the trust region strategy in the implementation of the Gauss–Newton method, which is another original contribution of this work. The combination of the damage function approach with the trust region strategy is a practical alternative to the pure mathematical regularization techniques such as Tikhonov approach. Afterwards the updating procedure is validated with a real application to a prestressed concrete bridge. The damage in the highway bridge is identified by updating the Young's and the shear modulus, whose distribution over the FE model are approximated by piecewise linear functions.

1. Introduction

Regular inspection and condition assessment of civil structures are necessary to allow early detection of any defect and to enable maintenance and repair works at the initial

*Corresponding author. Tel.: +32-16-321665; fax: +32-16-321988.
E-mail address: anne.teughels@bwk.kuleuven.ac.be (A. Teughels).
URL: http://www.kuleuven.ac.be/bwm/.

0022-460X/$ - see front matter © 2003 Elsevier Ltd. All rights reserved.
doi:10.1016/j.jsv.2003.10.041

damage phase, such that the structural safety and reliability is guaranteed with minimum costs.

Visual inspection has been the most common method used in detecting structural damage. But the increased size and complexity of today's structures reduce its efficiency. Conventional visual inspection can be costly and time consuming, especially when disassembly is necessary to provide access to the area being inspected. Furthermore, this technique is inadequate for identifying damage which is invisible to human eyes.

Non-destructive damage detection techniques, such as ultrasonic or acoustic methods, magnet field methods, X-ray inspection, etc. provide alternatives to detect occurrence of damage [1]. However, these are also local approaches and they require a prior knowledge of the location of the affected area and its accessibility.

On the other hand, the non-destructive detection methods that monitor the dynamic characteristics of the structure are appropriate since they provide a 'global' way to assess the structural state. These methods are based on the fact that the occurrence of damage in a structural system leads to changes in its dynamic properties (eigenfrequencies, mode shapes, modal damping rates and transfer functions). Dynamics-based damage identification methods have drawn world-wide attention and literature reviews have been provided by Doebling et al. [2] and Stubbs et al. [3]. Recently, an updated review has been produced which contains new technical developments published between 1996 and 2001 in the discipline of structural health monitoring [4]. An inverse problem is solved that consists of predicting the location and severity of the damage, given the structural dynamic characteristics before and after the damage.

The most common dynamic parameters used in damage detection, are eigenfrequencies and mode shapes. For example, Salawu [5] presents a review on the use of eigenfrequency changes for damage diagnostics. It is however hard to obtain spatial information of the structural damage from changes in only the eigenfrequencies and for this reason, mode shape information should also be used to uniquely localise the damage [6]. Ho and Ewins [7] present various methods of comparing mode shape information. Natke and Cempel [8] use changes in eigenfrequencies and mode shapes to detect damage in a cable-stayed steel bridge. Doebling and Farrar [9] examine if damage has produced a statistically significant change in the mode shapes.

However, a large number of measurement locations can be required to accurately characterize the mode shape vectors and to provide sufficient resolution for determining the damage location. As an alternative application of the mode shape information, Pandey et al. [10] introduced the use of mode shape curvatures and Maeck and De Roeck [11] extended this approach by using mode shape curvatures in a direct stiffness calculation technique, which they apply to damage identification in a prestressed concrete bridge. They use the changes in the dynamic stiffness, given by changes in the modal bending moment over the modal curvature, as an indicator for the presence of damage. Ho and Ewins [7] state that the derivatives of mode shapes are more sensitive to damage, but the differentiation process enhances the experimental errors inherent in mode shapes, yielding a large statistical uncertainty. The authors therefore propose changes in the squared mode shape slope as damage indicating features.

Kim et al. [12] evaluate damage detection and localization algorithms based on changes in eigenfrequencies, mode shapes and modal strain energy. Changes in strain energy are also used as a damage indicator by Cornwell et al. [13] and Yu et al. [14]; while Catbas and Aktan [15] and

Bernal [16] propose the use of the dynamically measured flexibility matrix for damage identification.

The dynamics-based methods can be classified into model based and non-model based approaches, depending on whether they use a numerical model or not. Damage identification by FE model updating belongs to the former group. An adequate FE model should be used that is able to predict the observed changes. Structural damage is represented by a decrease in the stiffness of the individual elements. In FE model updating the element stiffness properties are adjusted such that numerical and measured modal parameters correspond as closely as possible [17]. For damage identification, the procedure is performed in two updating processes. In the first the initial FE model is tuned to the undamaged structure, which is used as a reference model. In the second process the reference FE model is updated to obtain a model that can reproduce the experimental modal data of the damaged state. The damage is defined by means of correction factors with respect to the reference model. Brownjohn et al. [18] describe extensively the FE model updating technique applied to structural condition assessment of bridges.

The general methodology for FE model updating is known by the scientific community, however several practical implementations exist which all treat the ill-posedness of the inverse problem differently. In this article an improved updating procedure is proposed which is first explained theoretically and then applied to a real bridge structure, namely the Z24 bridge in Switzerland. It is a prestressed concrete bridge with three spans which is damaged by lowering one of the intermediate piers. Eigenfrequency as well as mode shape discrepancies are minimized, corresponding to the first four bending and/or torsion modes and the first transversal mode. The mode shape data are originally unscaled as they are obtained from ambient vibration tests and thus require an additional scaling operation. Both types of discrepancies are weighted with an appropriate factor in order to take their different levels of measurement noise into account. The updating parameters are both the Young's and the shear modulus of all the girder elements. A non-linear least squares problem is solved with a sensitivity based Gauss–Newton algorithm, which is made more robust by implementing it with a trust region strategy.

In order to improve the condition of the sensitivity matrix the number of unknown parameters is reduced by using a limited set of damage functions [19]. In particular, the girder stiffness distribution is approximated with a piecewise linear function and the parameters defining this function become the actual variables of the minimization problem. With this approach a realistic smooth result is always obtained. The method can be extended by including higher order functions.

A damage pattern of the bridge is identified that is consistent with the expected one. To compare, the results obtained by a technique that calculates the stiffness directly [20] are also given. Both techniques generate similar results.

2. General FE model updating procedure

2.1. Objective function

In FE model updating, an optimization problem is set up in which the differences between the experimental and numerical modal data have to be minimized by adjusting the uncertain model

properties [17]. In this paper the experimental eigenfrequencies ($\tilde{\nu}_j$) and mode shapes ($\tilde{\boldsymbol{\phi}}_j$) are used for the tuning. In civil engineering, the measurements are often obtained in operational conditions (ambient vibrations), which means that the exciting forces (coming from wind, traffic, etc.) are unknown. As a consequence, an absolute scaling of the mode shapes is missing. Furthermore, only the translation degrees of freedom of the mode shapes can be measured.

The minimization of the objective function is stated as a non-linear least squares problem:

$$\min_{\mathbf{p}} f(\mathbf{p}) = \tfrac{1}{2}||\mathbf{r}(\mathbf{p})||^2 = \frac{1}{2}\left|\left|\begin{matrix}\mathbf{r}_f(\mathbf{p})\\ \mathbf{r}_s(\mathbf{p})\end{matrix}\right|\right|^2, \quad \begin{matrix}\mathbf{r}_f : \mathbb{R}^n \to \mathbb{R}^{m_f}\\ \mathbf{r}_s : \mathbb{R}^n \to \mathbb{R}^{m_s}\end{matrix} \tag{1}$$

in which $||.||$ denotes the Euclidean norm. The residual vector $\mathbf{r} : \mathbb{R}^n \to \mathbb{R}^m$ contains the frequency residuals $\mathbf{r}_f$ and mode shape residuals $\mathbf{r}_s$ ($m = m_f + m_s$). The vector $\mathbf{p} \in \mathbb{R}^n$ represents the set of design variables. Both types of residuals can be formulated respectively as [19]

$$r_f(\mathbf{p}) = \frac{\lambda_j(\mathbf{p}) - \tilde{\lambda}_j}{\tilde{\lambda}_j}, \quad \text{with } \lambda_j = (2\pi\nu_j)^2, \tag{2}$$

$$r_s(\mathbf{p}) = \frac{\phi_j^l(\mathbf{p})}{\phi_j^r(\mathbf{p})} - \frac{\tilde{\phi}_j^l}{\tilde{\phi}_j^r}, \tag{3}$$

where l and r denote, respectively, an arbitrary and a reference degree of freedom of mode shape $\boldsymbol{\phi}_j$ (or $\tilde{\boldsymbol{\phi}}_j$) (Fig. 1).

Relative differences are taken in r_f in order to obtain a similar weight for each frequency residual. In r_s each mode shape component l is divided by a reference component r—which is a component with a large amplitude—since the numerical and experimental mode shapes can be scaled differently.

The least squares problem should be overdetermined, i.e. $m > n$, in order to obtain a unique solution. Otherwise—when more variables have to be determined than there are residuals available—there are infinitely many solutions and the minimum norm solution (defined with the Moore–Penrose pseudo-inverse [21] of the sensitivity matrix) can be sought, but according to Friswell and Mottershead [22] this rarely leads to physically meaningful updated parameters. Furthermore, by overdetermining the set, the influence of the measurement noise is minimized and an effective weighting of the residual functions—according to their importance and amount of noise—can be applied.

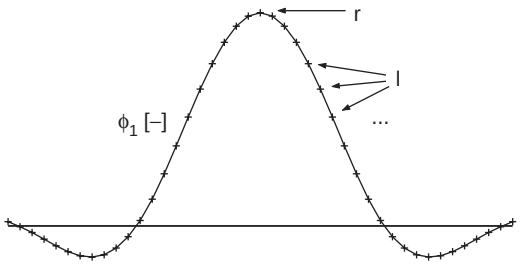

Fig. 1. Mode shape $\boldsymbol{\phi}_1$ with its components l and one reference component r.

Since the modal data (v and ϕ) are non-linear functions of the uncertain model properties, Eq. (1) is a non-linear least squares problem. It is solved with an iterative sensitivity based optimization method. The characteristics of the least squares problem can be exploited, namely the gradient and the Hessian of the objective function (Eq. (1)) have the following special structure:

$$\nabla f(\mathbf{p}) = \sum_{j=1}^{m} r_j(\mathbf{p}) \nabla r_j(\mathbf{p}) = \mathbf{J}_p(\mathbf{p})^{\mathrm{T}} \mathbf{r}(\mathbf{p}), \tag{4}$$

$$\nabla^2 f(\mathbf{p}) = \mathbf{J}_p(\mathbf{p})^{\mathrm{T}} \mathbf{J}_p(\mathbf{p}) + \sum_{j=1}^{m} r_j(\mathbf{p}) \nabla^2 r_j(\mathbf{p}) \approx \mathbf{J}_p(\mathbf{p})^{\mathrm{T}} \mathbf{J}_p(\mathbf{p}) \tag{5}$$

with $\mathbf{J}_p$ the Jacobian matrix (or sensitivity matrix), containing the first partial derivatives of the residuals r_j (r_f and r_s) with respect to $\mathbf{p}$. In the Gauss–Newton method [23], the Hessian is approximated with the first order term in Eq. (5), which is equivalent with solving the following linear least squares problem in each iteration k:

$$\min_{\mathbf{z}} \; q_k(\mathbf{z}) = \tfrac{1}{2} \|\mathbf{r}(\mathbf{p}_k) + \mathbf{J}(\mathbf{p}_k)\mathbf{z}\|^2, \quad \text{with } \mathbf{p}_{k+1} = \mathbf{p}_k + \mathbf{z}_k. \tag{6}$$

$q_k(\mathbf{z})$ is the quadratic model function that approximates $f(\mathbf{p})$ at the current vector $\mathbf{p}_k$; $\mathbf{z}$ denotes the step vector from $\mathbf{p}_k$.

In the paper, Matlab-software [23] is used to apply the Gauss–Newton method. Furthermore, the trust region implementation is chosen which causes the optimization process to converge. Namely, in order to prevent the iterates from taking extremely large steps in cases of bad function approximations, the algorithm determines in each iteration k a 'trust region' surrounding $\mathbf{p}_k$ where the model function q_k (in Eq. (6)) can be trusted. A candidate for the new iterate, $\mathbf{p}_{k+1} = \mathbf{p}_k + \mathbf{z}_k$, is then computed by approximately minimizing q_k inside the trust region. Thus Eq. (6) becomes

$$\min_{\mathbf{z}} \; q_k(\mathbf{z}) = \tfrac{1}{2} \|\mathbf{r}(\mathbf{p}_k) + \mathbf{J}(\mathbf{p}_k)\mathbf{z}\|^2, \tag{7}$$

where $\mathbf{z}$ lies inside the trust region.

If the candidate does not produce a sufficient decrease in f (i.e. the original objective function in Eq. (1))—which indicates that the model function q is an inadequate representation of f—the subproblem Eq. (7) is resolved with a smaller trust region. Otherwise the candidate is accepted as a new iterate from which the process reiterates. Since in this case the model function is generally reliable, the trust region might be increased.

Typically, the trust region is a sphere defined by $\|\mathbf{z}\| \leqslant \Delta$, where $\Delta > 0$ is called the trust region radius. The radius Δ_k is adjusted between iterations according to the agreement between predicted and actual reduction in the function f as measured by the ratio ρ_k:

$$\rho_k = \frac{f(\mathbf{p}_k) - f(\mathbf{p}_k + \mathbf{z}_k)}{f(\mathbf{p}_k) - q_k(\mathbf{z}_k)}. \tag{8}$$

If there is a good agreement ($\rho_k \approx 1$), then Δ_k is increased; if the agreement is poor (ρ_k small or ρ_k negative), then Δ_k is decreased, otherwise, Δ_k remains unchanged.

The decision to accept a step $\mathbf{z}_k$ is also based on ρ_k. Namely, the ratio ρ_k must exceed a small positive number (typically $\rho_k \geqslant 0.0001$). If this test fails, the step is recalculated with a smaller trust region. In general, the step direction changes whenever the size of the trust region is altered.

More information regarding the trust region approach can be found in Refs. [23–25]. In Matlab-software the trust region implementation is provided such that the algorithm can be performed automatically.

In FE model updating, the trust region strategy is an additional measure to improve the robustness of the updating procedure. The most effective measure to treat the ill-posedness of the inverse problem however is provided by the damage functions, as explained below.

2.2. *Design variables* **p**

One or more uncertain physical properties X (e.g. the Young's modulus) are updated in each element e of the numerical FE model. A dimensionless correction factor a^e expresses the relative difference of the updated value of property X with respect to its initial value X_0^e, in element e:

$$a^e = -\frac{X^e - X_0^e}{X_0^e} \quad \Rightarrow \quad X^e = X_0^e(1 - a^e). \tag{9}$$

The correction factors can affect one element or may be assigned to an element group. If the uncertain physical property is linearly related to the stiffness matrix of the element (group), one has:

$$\mathbf{K}^e = \mathbf{K}_0^e(1 - a^e), \tag{10}$$

$$\mathbf{K} = \mathbf{K}^u + \sum_{e=1}^{n_e} \mathbf{K}_0^e(1 - a^e), \tag{11}$$

where $\mathbf{K}_0^e$ and $\mathbf{K}^e$ are the initial and updated element stiffness matrix respectively, $\mathbf{K}$ is the global stiffness matrix and $\mathbf{K}^u$ is the stiffness matrix of the element (group) whose properties remain unchanged. n_e is the number of elements (groups) that are updated.

Adjusting the model property of all the elements separately would result in a high number of updating variables $\{a^e\}$, which causes the sensitivity matrix $\mathbf{J}$ to become ill-conditioned for the same residual vector $\mathbf{r}$. Furthermore, a physically meaningful optimization result is not guaranteed since neighbouring elements can be adjusted independently. Therefore, the distribution of the correction factors $\{a^e\}$—which define on their turn the distribution of the updated physical properties X over the FE model—is approximated by combining a limited set of global damage functions N_i [19].

The correction factor in element e is obtained with the following linear combination:

$$a^e = \sum_{i=1}^{n} p_i N_i(\mathbf{x}^e) \tag{12}$$

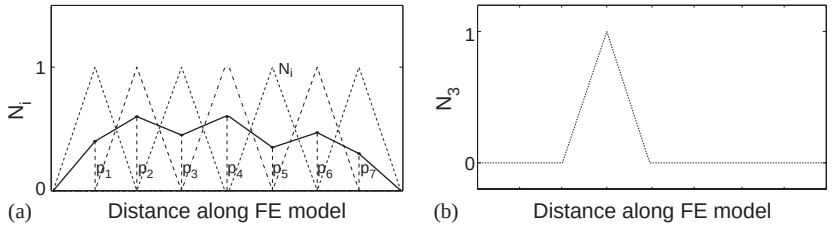

Fig. 2. Triangular-like damage functions N_i are used to approximate the distribution of the element correction factors a^e with a piecewise linear function: (a) continuous piecewise linear function (black) and set of seven triangular-like damage functions N_i (grey); (b) one isolated damage function.

with n the number of damage functions $N_i(\mathbf{x})$ ($n \ll n_e$); p_i their multiplication factor; and $\mathbf{x}^e$ the coordinates of the centre[1] of element e. The vector notation is

$$\mathbf{a}_{n_e \times 1} = [\mathbf{N}]_{n_e \times n} \ \mathbf{p}_{n \times 1} \tag{13}$$

or in full length:

$$\begin{Bmatrix} a^1 \\ a^2 \\ \vdots \\ a^{n_e} \end{Bmatrix} = \begin{bmatrix} N_1(\mathbf{x}^1) & \dots & N_n(\mathbf{x}^1) \\ N_1(\mathbf{x}^2) & \dots & N_n(\mathbf{x}^2) \\ \vdots & \dots & \vdots \\ N_1(\mathbf{x}^{n_e}) & \dots & N_n(\mathbf{x}^{n_e}) \end{bmatrix} \begin{Bmatrix} p_1 \\ p_2 \\ \vdots \\ p_n \end{Bmatrix}.$$

In this paper triangular-like damage functions N_i are used, varying between 0 and 1, such that a piecewise linear function is obtained to approximate the continuous distribution of the physical properties (Fig. 2). Analogously as shape functions in FE theory, the damage functions are defined on a mesh of damage elements, which in its turn is defined on top of the mesh of finite elements. The accuracy of the result is determined by the coarseness of the damage element mesh—rather than by the specific layout of the mesh—and it can be improved by refining the mesh, resulting in more linear pieces (damage elements) used to approximate the continuous distribution. Alternatively, higher order functions can also be used to improve the accuracy. Both means result in more unknown parameters p_i to be identified.

The damage functions can be used for subset selection, for example if no prior knowledge about the erroneous model parameters is available. Those regions (or damage elements) in the FE model are selected whose corresponding columns in the sensitivity matrix best represent the residual vector $\mathbf{r}$, analogously as the selection technique explained by Lallement and Piranda [26]. The FE model can then be further updated using a fine mesh of damage functions over the selected regions.

In the particular case of damage identification, first a coarse mesh can be used to locate the damage and simultaneously assess its severity in broad outlines. If required, a more detailed damage pattern can then be identified in a second updating process by correcting only the elements at the damaged zone using a finer mesh.

[1] By discretizing the continuous distribution in the centre points, the correction factor is taken constant for each element.

Each set of multiplication factors **p** defines all the updating parameters **a** in a unique sense, with the linear combination of Eq. (13). Therefore, the only unknown variables of the optimization problem are these multiplication factors **p**. Hence, this approach reduces the number of unknowns considerably, resulting in a robust optimization method. The identifiability of the design variables increases since the correction factors of several adjacent elements—that can have a similar effect on the modal data, especially on the mode shapes—are assembled by means of the damage functions. Furthermore, it always generates a smooth distribution of the model properties, generated by the piecewise linear function.

The combination of the damage function approach with the trust region implementation of the optimization algorithm provides an attractive alternative for the classical regularization techniques—such as Tikhonov or extended least squares—which can be too mathematical and rather artificial for practice usage. As opposed to the latter, physical interpretation can be attached to the damage functions which makes this approach easy to use in practice.

In addition to the trust region implementation, explicit bound constraints can also be applied, which have a favourable effect on the problem stability in the sense that they reduce the search space and consequently avoid divergence. Furthermore, physical limits can be imposed on the variables.

2.3. Sensitivity matrix

The modal sensitivities with respect to the correction factors a^e can be calculated using the formulas of Fox and Kapoor [27]. If only stiffness parameters have to be corrected, the formulas of Fox and Kapoor are simplified to

$$\frac{\partial \lambda_j}{\partial a^e} = \boldsymbol{\phi}_j^T \frac{\partial \mathbf{K}}{\partial a^e} \boldsymbol{\phi}_j \overset{\text{Eq. (11)}}{=} -\boldsymbol{\phi}_j^T \mathbf{K}_0^e \boldsymbol{\phi}_j \overset{\text{Eq. (10)}}{=} \boldsymbol{\phi}_j^T \frac{-\mathbf{K}^e}{(1-a^e)} \boldsymbol{\phi}_j = \frac{-\boldsymbol{\phi}_j^T \mathbf{F}_j^e}{(1-a^e)}, \tag{14}$$

$$\begin{aligned} \frac{\partial \boldsymbol{\phi}_j}{\partial a^e} &= \sum_{q=1;q\neq j}^{d} \frac{\boldsymbol{\phi}_q}{\lambda_j - \lambda_q} \left(\boldsymbol{\phi}_q^T \frac{\partial \mathbf{K}}{\partial a^e} \boldsymbol{\phi}_j \right) \overset{\text{Eq. (11)}}{=} \sum_{q=1;q\neq j}^{d} \frac{\boldsymbol{\phi}_q}{\lambda_j - \lambda_q} (-\boldsymbol{\phi}_q^T \mathbf{K}_0^e \boldsymbol{\phi}_j) \\ &= \sum_{q=1;q\neq j}^{d} \frac{\boldsymbol{\phi}_q}{(\lambda_j - \lambda_q)} \left(\frac{-\boldsymbol{\phi}_q^T \mathbf{F}_j^e}{1-a^e} \right), \end{aligned} \tag{15}$$

where $\mathbf{F}_j^e$ represents the forces at the nodes of element e corresponding to mode shape $\boldsymbol{\phi}_j$. The nodal displacements and forces are provided by any FE package, consequently the modal sensitivities can always be calculated by means of the formulae (14) and (15). Instead of the complete base (in Eq. (15) d denotes the analytical model order) a truncated base is used, which should be high enough in view of the condition of the sensitivity matrix. In the sensitivity expressions above the (analytical) mode shapes $\boldsymbol{\phi}$ are mass-normalized. In the residual vector, Eq. (3), however both the analytical and experimental mode shapes are scaled to one in the reference node. The expressions above can therefore not be used as such but require some modifications, as explained below.

The modal sensitivities (Eqs. (14) and (15)) are substituted in the sensitivities of the actual residuals r_j:

$$\frac{\partial r_f}{\partial a^e} = \frac{1}{\tilde{\lambda}_j}\frac{\partial \lambda_j}{\partial a^e}, \tag{16}$$

$$\frac{\partial r_s}{\partial a^e} = \frac{1}{\phi_j^r}\frac{\partial \phi_j^l}{\partial a^e} - \frac{\phi_j^l}{(\phi_j^r)^2}\frac{\partial \phi_j^r}{\partial a^e}, \tag{17}$$

which are used to calculate the sensitivity matrix $\mathbf{J}_a$ of the residual vector $\mathbf{r}$ with respect to the correction factors $\mathbf{a}$. In the optimization procedure, however, the sensitivities of $\mathbf{r}$ with respect to the design variables $\mathbf{p}$ are needed. Therefore, based on the mutual dependency between $\mathbf{a}$ and $\mathbf{p}$ expressed by Eq. (13), each component of the sensitivity matrix $\mathbf{J}_p$ is calculated as

$$\frac{\partial r_j}{\partial p_i} = \sum_{e=1}^{n_e} \frac{\partial r_j}{\partial a^e}\frac{\partial a^e}{\partial p_i} \overset{\text{Eq.(13)}}{=} \sum_{e=1}^{n_e} \frac{\partial r_j}{\partial a^e} N_i(\mathbf{x}^e), \tag{18}$$

in which Eqs. (16) and (17) have to be filled in. Equivalently, in matrix notation, one has

$$[\mathbf{J}_p]_{m\times n} = [\mathbf{J}_a]_{m\times n_e}[\mathbf{N}]_{n_e\times n}, \tag{19}$$

where $\mathbf{J}_p$ and $\mathbf{J}_a$ are the sensitivity matrices with respect to the design variables $\mathbf{p}$ and the element correction factors $\mathbf{a}$ respectively. $\mathbf{N}$ is the matrix containing the global damage functions.

2.4. Weighting

The least squares problem formulation allows the residuals to be weighted separately corresponding to their importance and amount of noise. The weight factors influence the result only in case of an overdetermined set of equations, i.e. more residuals than design variables and only the relative proportion of the weighting factors is important, not their absolute values. The following weighted least squares problem is solved

$$\min \tfrac{1}{2}\|\mathbf{W}^{1/2}\mathbf{r}(\mathbf{p})\|^2 \tag{20}$$

with $\mathbf{W}$ the weighting matrix. If the weighting matrix is a diagonal matrix, i.e. $\mathbf{W} = diag(\ldots, w_j^2, \ldots)$, Eq. (20) can be written equivalently as

$$\min \frac{1}{2}\sum_{j=1}^{m} [w_j r_j(\mathbf{p})]^2, \tag{21}$$

where w_j is the weighting factor of residual r_j.

Generally, the experimental eigenfrequencies are a good indicator for damage and can be measured quite accurately. However, it is difficult to detect zones of local damage using only eigenfrequencies. Mode shapes in their turn permit a more detailed prediction of the damage distribution, but the measurements are more noisy.

A well-known (statistical) approach is to choose the weighting matrix as the inverse of the covariance matrix of the experimental errors, which yields the minimum variance Gauss–Markov estimate [28]. However, in practice this statistical information is often not available such that the analyst has to rely on his engineering judgement in choosing the appropriate weights.

The eigenfrequency residuals, Eq. (2), are already equally weighted by their definition as relative differences and all the mode shape residuals, Eq. (3), are of the same order of magnitude, since the mode shape components vary between $+1$ and -1 due to the normalization in the reference node. Consequently, the analyst only has to make the right balance between both residual types according to their experimental accuracy, i.e. he has to choose the proper ratio w_s/w_f for the mode shape and eigenfrequency residuals or, equivalently, the proper w_s for unit w_f.

The appropriate balance can be obtained iteratively, by performing some trial runs: if for the obtained result the eigenfrequencies correspond fully but the mode shapes still show a considerable discrepancy, it can be assumed that too much weight is given to the frequency residuals; and vice versa, if a very non-smooth result is obtained—which refers to a too high influence from the mode shape measurement errors—and for which the eigenfrequency residuals are not minimized well, the weight for the mode shapes should be decreased. A more systematic approach—similar to the L-curve method for Tikhonov regularization techniques [22]—would be possible, consisting of plotting the norms of both residual vectors, $\mathbf{r}_f$ and $\mathbf{r}_s$, for different weighting factors w_s and then selecting the most optimum point. However this would require many more simulations.

3. Damage detection of bridge Z24

3.1. Structure, experimental data and FE model

3.1.1. Structure

The FE model updating technique is applied to identify the damage of the highway bridge Z24 in Switzerland. It is a prestressed concrete bridge with three spans, supported by two intermediate piers and a set of three columns at each end (Fig. 3a and b). Both types of supports are rotated with respect to the longitudinal axis which results in a skew bridge. The overall length is 58 m.

3.1.2. Experimental data

In the framework of the Brite EuRam Programme CT96 0277 SIMCES, the bridge is progressively damaged in a number of damage scenarios [20,29] which are listed in Table 1. A full description of the damage scenarios can be found in [30]. The damage scenario considered in this paper consists of the lowering of one of the supporting piers (at 44 m) by 95 mm (no. 6 in Table 1), inducing cracks in the bridge girder above this pier. It simulates the settlement of the pier foundation.

The modal data are identified from ambient vibrations, before and after applying the damage. The measurements are performed in operational conditions, in particular the measured vibrations are induced by the traffic of the highway underneath the bridge. The stochastic subspace technique [31] is used to extract the modal data from the vibration data. Accelerometers are placed on the bridge deck along three parallel measurement lines: at the centreline and along both sidelines (Fig. 3b). Nine measurement set-ups are used to measure the mode shapes.

The first five identified eigenmodes are used for the updating. The eigenfrequencies are given in Table 2. The average relative standard deviation of the experimental eigenfrequencies, $\sum_{j=1}^{5}\sigma_{vj}/\tilde{v}_j$, is around 0.7% for the undamaged as well as for the damaged bridge. The experimental mode

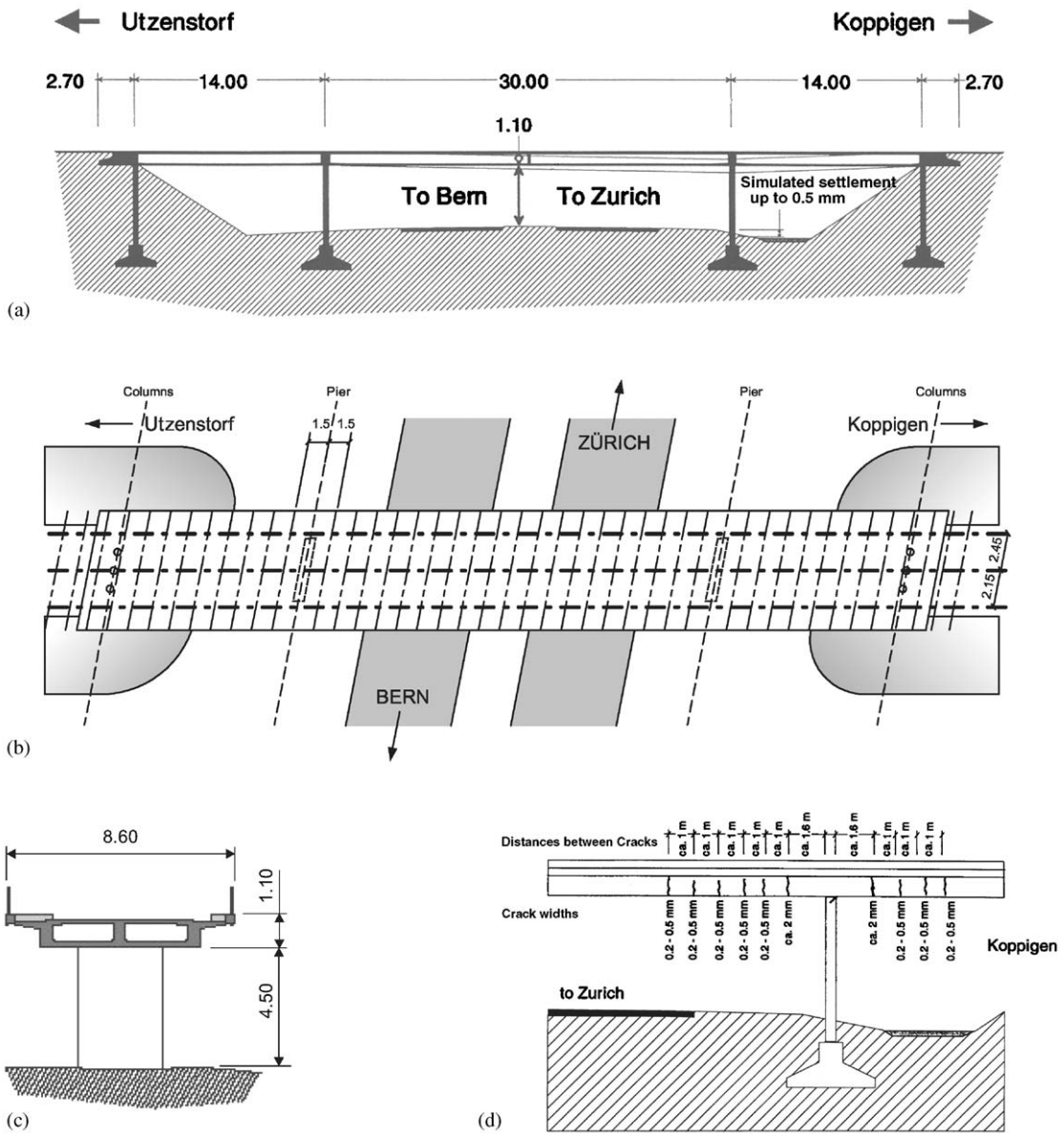

Fig. 3. Highway bridge Z24, Switzerland: (a) Elevation, (b) top view with measurement grid indicated and (c) cross-section of the bridge. (d) Cracks in the bridge girder, above the lowered pier (at 44 m).

shapes are obtained by glueing the parts that are identified in each setup using four reference channels. As a result, the standard deviation of the mode shapes can hardly be derived. The mode shapes are plotted in Fig. 4. The first and the fifth are pure bending modes, the third and fourth are coupled bending and torsional modes—due to the skewness of the bridge—and the second is a

Table 1
Damage scenarios on bridge Z24 [20]

No.	Scenario	Description/simulation of real damage cause
1	First reference measurement	Initial (healthy) structure
2	Second reference measurement	After installation of lowering system
3	Lowering of pier, 20 mm	Settlement of subsoil, erosion
4	Lowering of pier, 40 mm	
5	Lowering of pier, 80 mm	
6	Lowering of pier, 95 mm	
7	Tilt of foundation	Settlement of subsoil, erosion
8	Third reference measurement	After lifting of bridge to its initial position
9	Spalling of concrete, 12 m^2	Vehicle impact, carbonization and
10	Spalling of concrete, 24 m^2	subsequent corrosion of reinforcement
11	Landslide at abutment	Heavy rainfall, erosion
12	Failure of concrete hinge	Chloride attack, corrosion
13	Failure of anchor heads I	Corrosion, overstress
14	Failure of anchor heads II	
15	Rupture of tendons I	Erroneous or forgotten injection of
16	Rupture of tendons II	tendon tubes, chloride influence
17	Rupture of tendons III	

Table 2
Experimental, initial and updated eigenfrequencies and *MAC* values for the undamaged and damaged bridge Z24

Mode	Undamaged			Damaged		
	Experimental	FE model		Experimental	FE model	
		Initial	Updated		Reference	Updated
	Eigenfrequencies (Hz)			Eigenfrequencies (Hz)		
1	3.89	3.73	3.87	3.67	3.87	3.65
2	5.02	5.14	5.03	4.95	5.03	4.86
3	9.80	9.64	9.72	9.21	9.72	9.12
4	10.30	10.25	10.31	9.69	10.31	9.73
5	12.67	12.52	12.81	12.03	12.81	12.16
		MAC values (%)			*MAC* values (%)	
1		99.95	99.95		99.85	99.89
2		99.80	99.82		97.16	97.39
3		94.42	98.99		89.02	98.17
4		96.85	99.44		84.66	93.30
5		96.18	96.61		86.61	97.56

transversal mode. The settlement of the pier causes a change in mode shapes 3–5, due to the induced cracks in the bridge girder. It is the aim to detect, localize and quantify the damage pattern by adjusting the stiffness of the bridge girder.

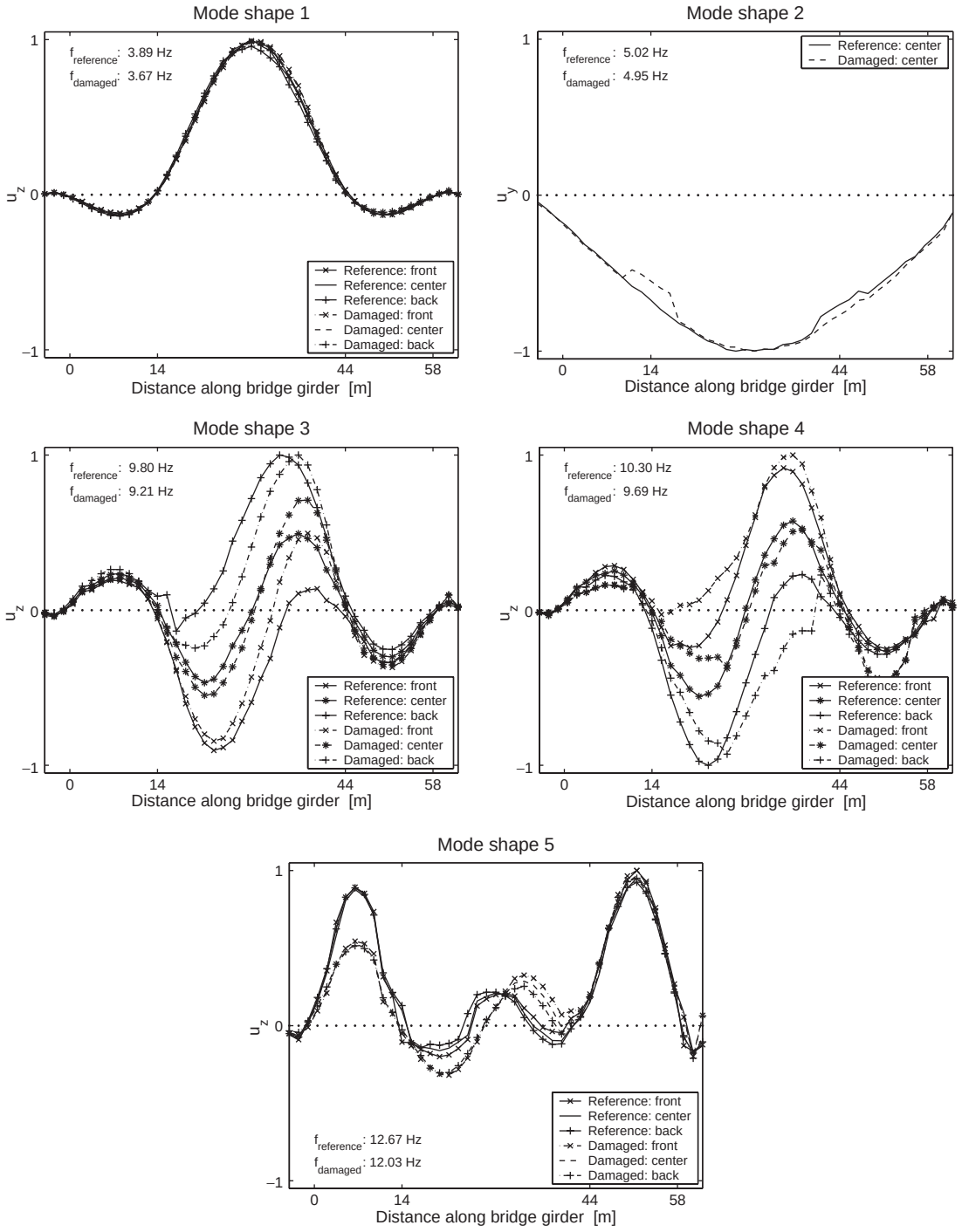

Fig. 4. Experimental eigenfrequencies and mode shapes of the bridge Z24 before and after lowering the pier. In the plots the front- and backline are shifted such that the measurement points on the three lines coincide. (X, Y, Z: longitudinal, transversal and vertical axes).

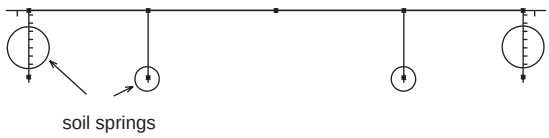

Fig. 5. FE model of the bridge in which the beam elements of the girder (82 elements) are updated. The soil springs at the supports are indicated (circles).

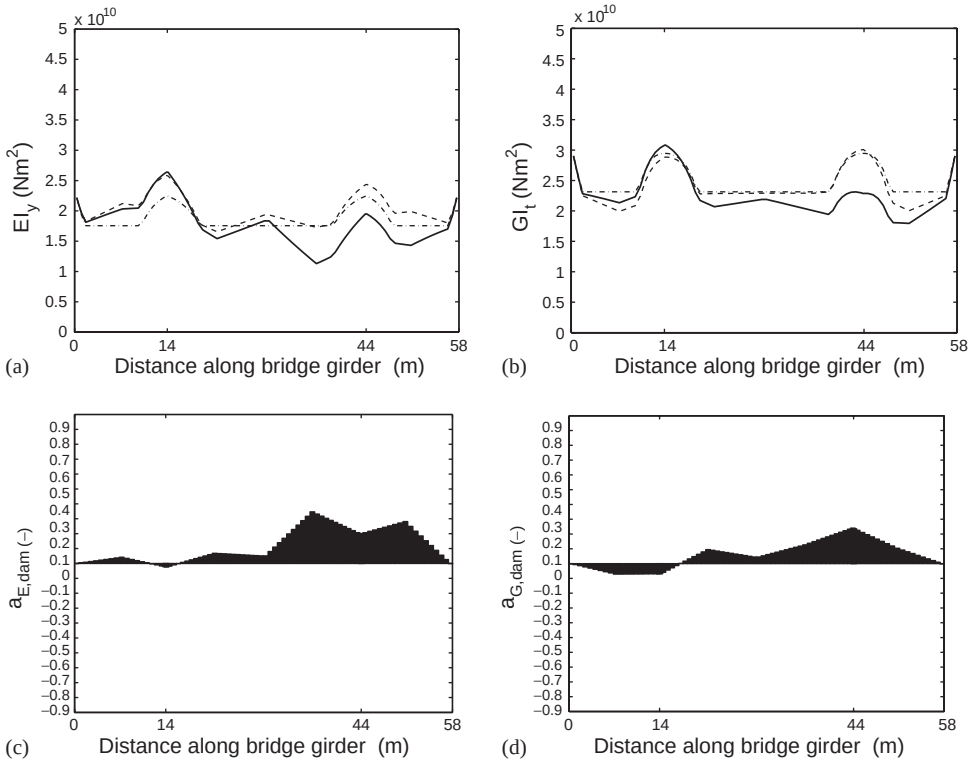

Fig. 6. Identified parameters: (a) bending stiffness distribution $EI_{\text{dam}} = EI_{\text{ref}}(1 - a_{E,\text{dam}})$ and (b) torsional stiffness distribution $GI_{t,\text{dam}} = GI_{t,\text{ref}}(1 - a_{G,\text{dam}})$. Dashed-dotted line: initial stiffness; dashed line: stiffness updated to undamaged state; solid line: stiffness updated to damaged state. The correction factors for the damaged bridge are given in: (c) $\mathbf{a}_{E,\text{dam}}$ and (d) $\mathbf{a}_{G,\text{dam}}$.

3.1.3. FE model

The bridge is modelled with a beam model (six degrees of freedom (d.o.f.s) in each node, three-dimensional) in ANSYS [32] (Fig. 5). Equivalent values for the cross-sectional area, the bending and torsional moment of inertia of the box section of the main girder (Fig. 3c) are calculated. The girder has higher stiffness values above the supporting piers (Fig. 6a and b) because of an increased thickness of bottom and top slab. Eighty-two beam elements are used to model the girder.

The piers and the columns at the abutments are modelled in a similar way. The principal axes of the piers are rotated to model the skewness of the bridge. The width of the piers is taken into account by means of specific constraint equations. Forty-four beam elements are used to model the piers, the columns and the abutments.

The concrete is considered to be homogeneous, with an initial value for the Young's modulus of $E_0 = 37.5$ GPa and $G_0 = 16$ GPa for the shear modulus.

Mass elements are used for the cross girders and foundations. Concentrated translational mass as well as rotary inertial components are considered.

In order to account for the influence of the soil, springs are included at the pier and column foundations, at the end abutments and around the columns (Fig. 5). The initial values of the soil stiffness are taken as: $K_{v,p} = 180 \times 10^6$ N/m^3, $K_{h,p} = 210 \times 10^6$ N/m^3 (under piers, at $x = 14$ and 44 m); $K_{v,c} = K_{h,c} = 100 \times 10^6$ N/m^3 (under columns, at $x = 0$ and 58 m); $K_{v,a} = 180 \times 10^6$ N/m^3, $K_{h,a} = 200 \times 10^6$ N/m^3 (at abutments) and $K_{v,ac} = K_{h,ac} = 100 \times 10^6$ N/m^3 (around columns).

The eigenfrequencies calculated with the initial FE model are listed in Table 2.

3.2. FE model updating: problem definition

3.2.1. Variables of the updating process

Two updating processes are performed, in order to model the reference and the damaged state of the bridge respectively.

The bending as well as the torsional stiffness of the beam elements of the girder are updated since the identified modes contain, besides pure bending, also coupled bending–torsion modes. They are adjusted by correcting the Young's and the shear modulus, E and G, respectively,

$$a_E^e = -\frac{E^e - E_{ref}^e}{E_{ref}^e} \quad \Rightarrow \quad E^e = E_{ref}^e(1 - a_E^e), \tag{22}$$

$$a_G^e = -\frac{G^e - G_{ref}^e}{G_{ref}^e} \quad \Rightarrow \quad G^e = G_{ref}^e(1 - a_G^e). \tag{23}$$

Both properties can be updated separately by using the appropriate DOFs in formulas (14) and (15), namely $\{u_x, u_y, u_z, rot_y, rot_z\}$ for the bending stiffness and $\{rot_{xx}\}$ for the torsional stiffness. The reference values, E_{ref}^e and G_{ref}^e, are the initial FE values in the first updating process, and in the second updating process are the identified values from the first updating process.

In the first updating process additionally the vertical soil stiffness under the supporting piers, $K_{v,p}$, and the horizontal soil stiffness under the end abutments, $K_{h,a}$, are updated. The former influences mainly the second and the fifth mode (transversal and bending), the latter only the second mode. The other soil stiffness values do not influence the considered modal data. Since the soil springs are not altered by the damage application they are not updated in the second updating process.

3.2.2. Damage functions

The bridge girder is subdivided into eight damage elements. Two (identical) piecewise linear damage functions are used for identifying the bending and the torsional stiffness distribution

respectively. Such a function is plotted in Fig. 2a, with the X-axis denoting the distance along the bridge girder.

In the first updating process the optimization problem contains 16 ($= 2 \times 7 + 2$) design variables, corresponding to the multiplication factors of both sets of damage functions, $\mathbf{p}_{E,i}$ and $\mathbf{p}_{G,i}$ (2×7), and the two correction factors for the soil springs. In the second process only 14 ($= 2 \times 7$) variables have to be identified, $\mathbf{p}_{E,i}$ and $\mathbf{p}_{G,i}$. They define the correction factors, $\mathbf{a}_E$ and $\mathbf{a}_G$ (2×82), in a unique sense by

$$a_E = \sum_{i=1}^{7} p_{E,i} N_i, \tag{24}$$

$$a_G = \sum_{i=1}^{7} p_{G,i} N_i. \tag{25}$$

The initial values for $\mathbf{p}$ in both processes are set to zero, corresponding to zero initial correction factors $\mathbf{a}$ over the whole girder length. The outer values of the piecewise linear damage function are restrained to zero, because the sensitivities at the ends of the beam are very low.

3.2.3. Objective function

The four vertical modes (bending and bending–torsion) and the transverse mode of the undamaged bridge are used to update the initial FE model to the reference undamaged state of the bridge. The latter mode is included in the process in order to identify the stiffness of the soil springs.

The residual vector in the updating process contains five frequency residuals r_f (2) and 492 mode shape residuals r_s (3). The vertical displacements u_z along the three measurement lines ($\pm 3 \times 39$ points) and the horizontal displacements u_y along the centreline (31 points) are used for the vertical and transversal modes respectively. Only the well measured displacements are selected. The total residual vector $\mathbf{r}$ (1) contains $m = 497$ residuals.

For the identification of the damaged zone only the four bending modes are used, measured on the bridge after the pier settlement. The transversal mode is not used since the soil springs are not updated in this process.

The residual vector in the second updating process contains four frequency residuals r_f and 451 mode shape residuals[2] r_s, which results in $m = 455$ residuals.

In both processes a weighting factor $w_s = \frac{1}{10}$ is applied in (Eq. (21)) to the mode shape residuals.

The least squares problem is solved with the trust region Gauss–Newton method.

3.3. Updating results

3.3.1. Identified parameters

The updated values of the vertical soil stiffness under the piers and the horizontal stiffness under abutments are: $K_{v,p} = 157 \times 10^6$ N/m^3 and $K_{h,a} = 145 \times 10^6$ N/m^3. These values are used in the FE model when identifying the damage.

[2] The selected displacements are plotted in Fig. 10 for the damaged bridge.

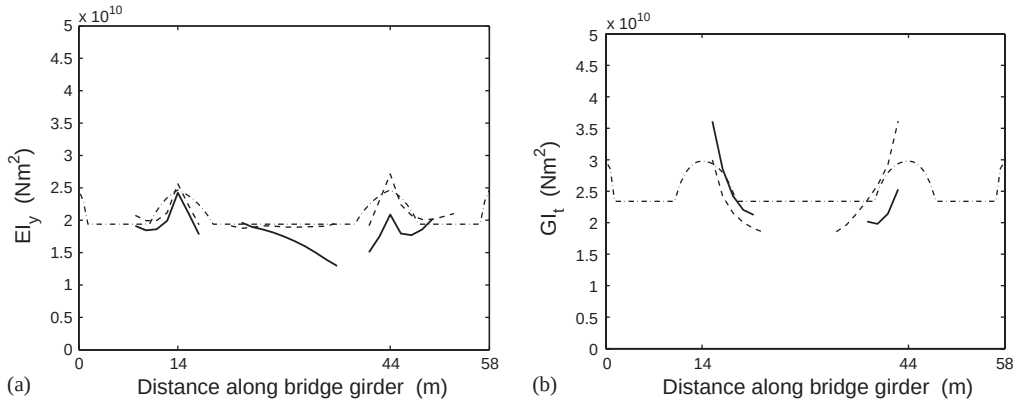

Fig. 7. Results obtained with the direct stiffness calculation (DSC) method: (a) bending stiffness distribution EI_y and (b) torsional stiffness distribution GI_t. Dashed-dotted line: initial stiffness; dashed line: identified stiffness for the undamaged state; solid line: identified stiffness for the damaged state. Note that in (b) the damage state corresponding to a pier settlement of 80 mm (scenario 5 in Table 1) instead of 95 mm is considered.

The stiffness distribution of the bridge girder—for bending as well as for torsion—is plotted in Fig. 6a and b. The initial and the updated values for the reference and damaged state are shown.

The reference state is characterized by a symmetrical stiffness pattern. The initial bending stiffness is increased above both piers, at the side spans and slightly in the middle of the bridge.

In the damaged state a decrease in the girder stiffness above the pier at 44 m, is clearly visible. This decrease is due to the lowering of the pier, which induced cracks in the beam girder at that location (Fig. 3d). The corresponding identified damage pattern, defined by the reduction factors $\mathbf{a}_E$ and $\mathbf{a}_G$, is plotted in Fig. 6c and d. The bending and the torsional stiffness are reduced with a maximum of 35% and 24% respectively, located in the expected cracked zone.

Some inaccuracies occur at the left side of the bridge girder—e.g. a non-physical increase in torsional stiffness—and are due to the coarseness of the damage functions, the measurement errors and the modelling assumptions. The fact is that a beam model is used, which is not able to model the structural behaviour of the box girder exactly (no modelling of restrained warping, shear lag effects, etc.).

In a computationally more expensive calculation, a more detailed damage pattern could be obtained using an FE model with solid elements and a finer mesh of (three-dimensional) damage functions. The higher number of unknowns in their turn require a larger set of noise-free experimental modal data.

3.3.2. *Comparison with direct stiffness calculation*

In Ref. [20] Maeck calculates the stiffness distribution with the DSC technique. In this technique the stiffness is calculated directly by dividing the modal internal forces (calculated with the measured eigenfrequencies and the mass distribution) by the measured curvatures of the mode shapes, so without updating a FE model. The bending and torsional stiffness[3] are plotted in

[3] The torsional stiffness is identified for the damage state corresponding to a pier settlement of 80 mm instead of 95 mm. Note that different initial values are used in Figs. 6a and 7a.

Fig. 7. The bending stiffness obtained with both methods, model updating and DSC, corresponds in broad outlines. The reduction in torsional stiffness above the settled pier is also identified with the DSC method. Again some anomalies appear in the identification of this property (e.g. an increase in GI_t above the left pier), because in this calculation a beam model is also used.

3.3.3. Modal data

Table 2 lists the initial and updated eigendata for the undamaged as well as for the damaged bridge. In the former all the five modes are used in the updating process, whereas in the latter only the bending modes (nos. 1, 3, 4, 5) are used.

By updating the initial FE model to the reference state, the eigenfrequencies correspond globally better with the experimental values (Fig. 8). In particular, the correction of the soil springs reduces the eigenfrequency difference of the transversal mode. For the mode shapes, a

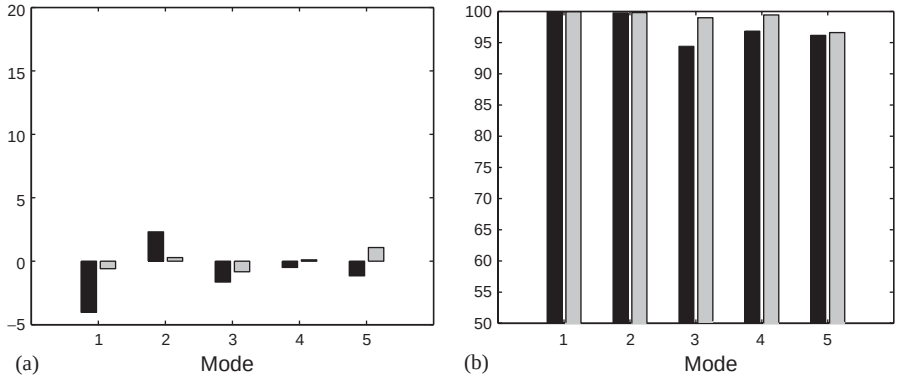

Fig. 8. Comparison between numerical and experimental modal data for the undamaged bridge: (a) relative eigenfrequency differences: $(\nu - \tilde{\nu})/\tilde{\nu}$ (%) and (b) *MAC* values: $|\boldsymbol{\phi}^{\mathrm{T}}\tilde{\boldsymbol{\phi}}|^2/(\boldsymbol{\phi}^{\mathrm{T}}\boldsymbol{\phi})(\tilde{\boldsymbol{\phi}}^{\mathrm{T}}\tilde{\boldsymbol{\phi}})$ (%).

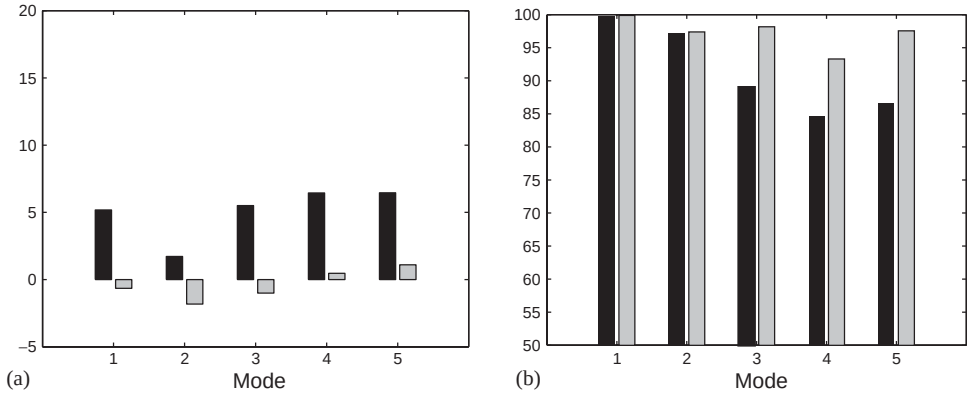

Fig. 9. Comparison between numerical and experimental modal data for the damaged bridge: (a) relative eigenfrequency differences: $(\nu - \tilde{\nu})/\tilde{\nu}$ (%) and (b) *MAC* values: $|\boldsymbol{\phi}^{\mathrm{T}}\tilde{\boldsymbol{\phi}}|^2/(\boldsymbol{\phi}^{\mathrm{T}}\boldsymbol{\phi})(\tilde{\boldsymbol{\phi}}^{\mathrm{T}}\tilde{\boldsymbol{\phi}})$ (%). The transversal mode (mode 2) is not used for the identification of the damage pattern (the second updating process).

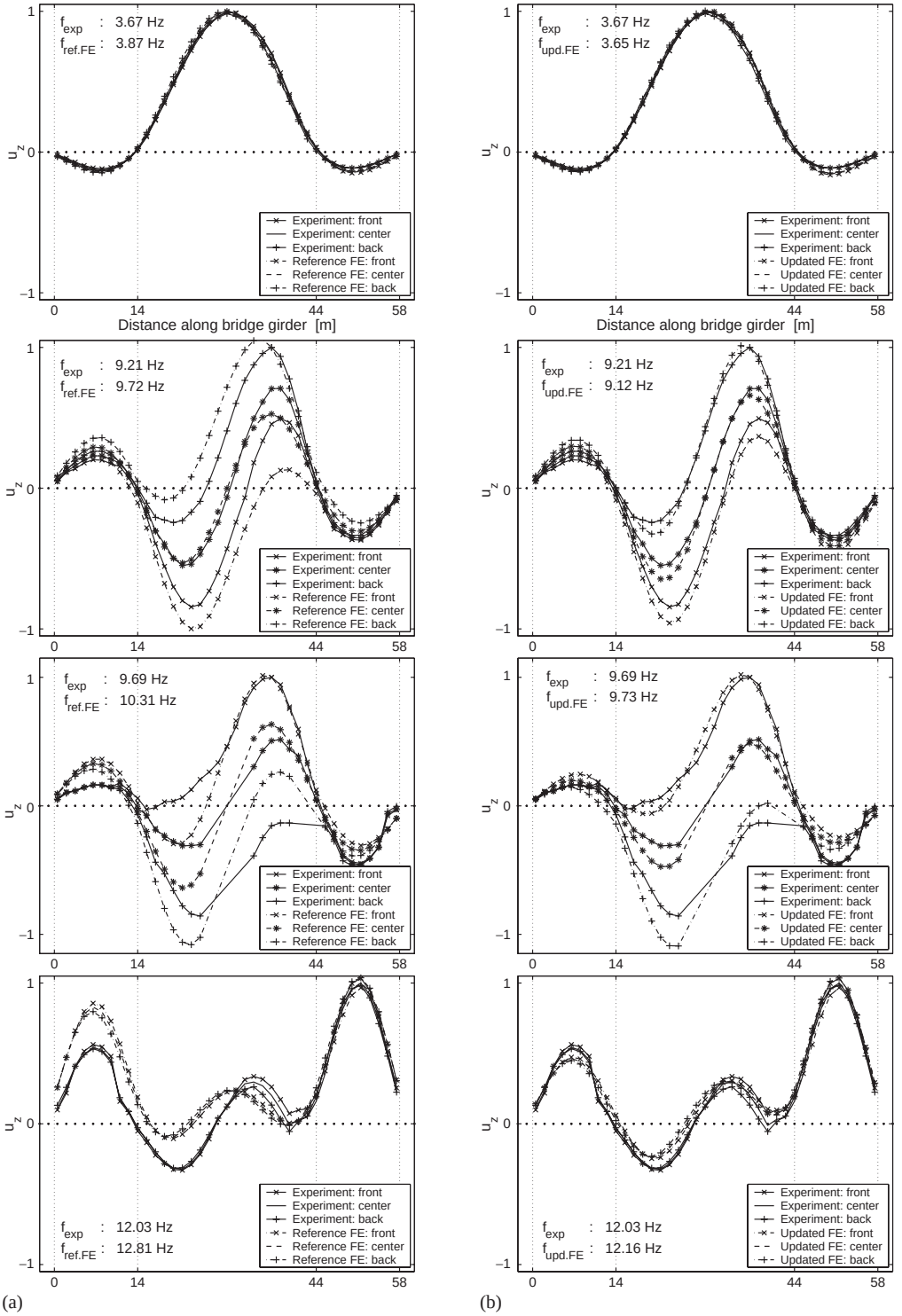

Fig. 10. Initial (a) and updated (b) numerical modes (nos. 1, 3, 4, 5) of the damaged bridge, to be compared with the experimental values.

clear improvement of the correlation can be observed, which is quantified by the MAC values, $MAC = |\boldsymbol{\phi}_j^{\mathrm{T}}\tilde{\boldsymbol{\phi}}_j|^2/(\boldsymbol{\phi}_j^{\mathrm{T}}\boldsymbol{\phi}_j)(\tilde{\boldsymbol{\phi}}_j^{\mathrm{T}}\tilde{\boldsymbol{\phi}}_j)$ [$\tilde{\boldsymbol{\phi}}$:experimental value]. Especially both coupled bending–torsion modes (nos. 3, 4) are improved considerably.

Also for the damaged bridge, the correlation between the numerical and experimental eigenfrequencies is improved very well with the updated FE model (Fig. 9). The updated numerical mode shapes clearly correspond better with the experimental mode shapes. However, the MAC value for the fourth mode shape remains under 95%, which is partially due to the bad quality of the experimental data of this mode shape (Fig. 10), due to the 'on site' measurements.

The initial and updated mode shapes for the damaged bridge are plotted in Fig. 10. The improvement in correspondence with the experimental values is clear.

4. Conclusions

An FE model updating method using modal data is presented. The updating procedure can be regarded as a parameter identification technique which aims to fit the unknown parameters of an analytical model such that the model behaviour corresponds as closely as possible to the measured behaviour. The general sensitivity based model updating method is improved by the use of damage functions and the trust region approach. The former measure is meant to improve the problem condition, the latter additionally stabilizes the optimization method.

The method is applied to a real civil structure, namely the highway bridge Z24 in Switzerland. Its damage pattern is identified using the eigenfrequencies and unscaled mode shape data obtained from ambient vibrations. The damage is represented by a reduction in bending and torsion stiffness of the bridge girder. For both properties a realistic damage pattern is identified and a good correspondence with the results of the direct stiffness calculation method is obtained.

For the undamaged as well as for the damaged bridge, the updated numerical modal data correspond well with the experimental data. By updating the soil stiffness in the first updating process, also the correlation for the transversal mode is improved.

Acknowledgements

Teughels A is a research assistant supported by a grant of the National Fund for Scientific Research (FWO—Flanders).

References

[1] J.E. Doherty, Nondestructive evaluation, in: A.S. Kobayashi (Ed.), *Handbook on Experimental Mechanics*, Prentice-Hall, New York, 1987 (Chapter 12).

[2] S.W. Doebling, C.R. Farrar, M.B. Prime, A summary review of vibration-based damage identification methods, *The Shock and Vibration Digest* 30 (2) (1998) 91–105.

[3] N. Stubbs, C. Sikorsky, S. Park, S. Choi, R. Bolton, A methodology to nondestructively evaluate the structural properties of bridges, in: *Proceedings of IMAC 17 International Modal Analysis Conference*, Kissimmee, FL, 1999, pp. 1260–1268.

[4] H. Sohn, C.R. Farrar, F.M. Hemez, et al., A review of structural health monitoring literature: 1996–2001, Technical Report Annex to SAMCO Summer Academy, Los Alamos National Laboratory, Cambridge, 2003.
[5] O.S. Salawu, Detection of structural damage through changes in frequency: a review, *Engineering Structures* 19 (9) (1997) 718–723.
[6] W.-X. Ren, G. De Roeck, Structural damage identification using modal data. I: simulation verification, *Journal of Structural Engineering* 128 (1) (2002) 87–95.
[7] Y.K. Ho, D.J. Ewins, On structural damage identification with mode shapes, in: *Proceedings of COST F3 Conference on System Identification and Structural Health Monitoring*, Madrid, Spain, 2000, pp. 677–686.
[8] H.G. Natke, C. Cempel, Model-aided diagnosis based on symptoms, in: *Proceedings of DAMAS 97*, Sheffield, UK, 1997, pp. 363–375.
[9] S.W. Doebling, C.R. Farrar, Using statistical analysis to enhance modal-based damage identification, in: *Proceedings of DAMAS 97*, Sheffield, UK, 1997, pp. 199–210.
[10] A.K. Pandey, M. Biswas, M.M. Samman, Damage detection from changes in curvature mode shapes, *Journal of Sound and Vibration* 145 (2) (1991) 321–332.
[11] J. Maeck, G. De Roeck, Damage detection on a prestressed concrete bridge and RC beams using dynamic system identification, in: *Proceedings DAMAS 99*, Trans Tech Publications, Dublin, Ireland, 1999, pp. 320–327.
[12] J.-T. Kim, Y.-S. Ryu, H.-M. Cho, et al., Damage identification in beam-type structures: frequency-based method vs mode-shape-based method, *Engineering Structures* 25 (1) (2003) 57–67.
[13] P. Cornwell, S.W. Doebling, C.R. Farrar, Application of the strain energy damage detection method to plate-like structures, in: *Proceedings of IMAC 15: International Modal Analysis Conference*, Orlando, FL, 1997, pp. 1312–1318.
[14] L. Yu, S.S. Law, M. Link, L.M. Zhang, Damage detection in bolted joint structures using element contribution on modal strain energy, in: *Proceedings of Second International Conference on Identification in Engineering System*, Swansea, 1999, pp. 516–526.
[15] F.N. Catbas, A.E. Aktan, Modal analysis for damage identification: past experiences and Swiss Z-24 bridge, in: *Proceedings of IMAC 20: International Modal Analysis Conference*, Los Angeles, CA, 2002, pp. 448–456.
[16] D. Bernal, Extracting flexibility matrices from state-space realizations, in: *Proceedings of COST F3 Conference on System Identification and Structural Health Monitoring*, Madrid, Spain, 2000, pp. 127–135.
[17] M.I. Friswell, J.E. Mottershead, *Finite Element Model Updating in Structural Dynamics*, Kluwer Academic Publishers, Dordrecht, The Netherlands, 1995.
[18] J.M.W. Brownjohn, P.-Q. Xia, H. Hao, Y. Xia, Civil structure condition assessment by FE model updating: methodology and case studies, *Finite Elements in Analysis and Design* 37 (2001) 761–775.
[19] A. Teughels, J. Maeck, G. De Roeck, Damage assessment by FE model updating using damage functions, *Computers and Structures* 80 (25) (2002) 1869–1879.
[20] J. Maeck, Damage Assessment of Civil Engineering Structures by Vibration Monitoring, Ph.D. Thesis, K.U. Leuven, Belgium, 2003.
[21] N.M.M. Maia, J.M.M. Silva, J. He, et al., *Theoretical and Experimental Modal Analysis*, Research Studies Press, Somerset, England, 1997.
[22] M.I. Friswell, J.E. Mottershead, Physical understanding of structures by model updating, in: *Proceedings of COST F3 International Conference on Structural System Identification*, Kassel, Germany, 2001, pp. 81–96.
[23] MATLAB, Version 2.1 (Release 12.1), *Matlab Optimization Toolbox User's Guide*, http://www.mathworks.com/products/optimization/, the Mathworks (2000).
[24] J. Nocedal, S.J. Wright, *Numerical Optimization*, Springer, New York, 1999.
[25] A.R. Conn, N.I.M. Gould, P.L. Toint, *Trust-Region Methods*, SIAM and Mathematical Programming Society, Philadelphia, 2000.
[26] G. Lallement, J. Piranda, Localisation methods for parameter updating of finite element models in elastodynamics, in: *Proceedings of Imac VIII*: *Eighth International Modal Analysis Conference*, Orlando, FL, 1990, pp. 579–585.
[27] R. Fox, M. Kapoor, Rate of change of eigenvalues and eigenvectors, *AIAA Journal* 6 (1968) 2426–2429.
[28] J.V. Beck, K.J. Arnold, *Parameter Estimation in Engineering and Science*, Wiley, New York, 1977.

[29] J. Maeck, G. De Roeck, Description of Z24 benchmark, *Mechanical Systems and Signal Processing* 71 (1) (2003) 127–131.
[30] C. Kramer, C.A.M. De Smet, G. De Roeck, Z24 bridge damage detection tests, in: *Proceedings of IMAC 17: International Modal Analysis Conference*, Kissimmee, Florida, USA, 1999.
[31] B. Peeters, G. De Roeck, Reference-based stochastic subspace identification for output-only modal analysis, *Mechanical Systems and Signal Processing* 6 (3) (1999) 855–878.
[32] ANSYS, Robust Simulation and Analysis Software, http://www.ansys.com/, Release 6.1, ANSYS Incorporated (2003).